Static Configurations of Free Liquid Surfaces in Low-gravity Environment

Tsukasa Nakayama

Department of Mechanical Engineering, Chuo University, Tokyo, Japan

1. Introduction

In space vehicles and artificial satellites, liquids having various functions are carried, as exemplified by coolants, fuels and so forth, and they constitute a substantial part of the total weight of spacecraft. The acceleration of a spacecraft due to a thrust causes the liquid in a container to move. Then, the moving liquid exerts forces and torques on the spacecraft. Therefore, in order to control the motion of spacecraft precisely and stabilize it, the knowledge of the liquid motion in moving containers, or sloshing, under low gravity is required.

The problem of liquid sloshing is formulated mathematically as an initial-boundary value problem and requires a static configuration of a free liquid surface as a part of initial conditions. As is well known, the static shape of a free surface is highly curved due to surface tension effects under low-gravity conditions. The curved free surface, called "meniscus", is governed theoretically by the Young-Laplace equation, for which several numerical methods have been developed in the past.[1-5] Among those methods, one developed by Concus et al.[2] is straightforward and easy to use. In the method, the Young-Laplace equation is transformed into a system of four ordinary differential equations and integrated numerically under well-posed initial conditions and a contact-angle condition. The system of differential equations includes a constant. Its value is not known *a priori* and must be determined as a part of solutions when the liquid vloume in a container is to be prescribed. However, Concus et al. have not shown any detailed way to evaluate the constant in their paper, and moreover the characteristic of the solution obtained by their method is not obvious.

Then, the present paper aims to make the characteristic of the method of Concus et al. clear and to develop a practical method for the evaluation of the constant. The method is used in the calculation of the meniscus configurations in two-dimensional rectangular, three-dimensional circular cylindrical and spheroidal containers. The numerical results are compared with analytical exact solutions wherever possible. Furthermore, the method is applied to the computation of configurations of droplets lying on horizontal flat plates.

2. Mathematical Formulation of the Problem

We consider a spheroidal container shown in Fig. 1 which is partially filled with an incompressible liquid. The liquid occupies a simply connected domain, and the remainder of the container is filled with a gas or a vapor. The container and the fluids in it are at rest in low-gravity environments. Our task is to find the configuration of the equilibrium interface (meniscus) between the liquid and the gas.

The meniscus is denoted by S_f and the wetted part of the impermiable container wall is denoted by S_w. The meniscus S_f is assumed to be smooth and meets the wall in a constant contact angle γ. The contact line at which the meniscus meets the wall is denoted by C. A cylindrical coordinate system (r, θ, z) is introduced and fixed to the container as partly shown in Fig. 1. The origin O is located at the center of the container. The z-axis coincides with the axis of rotational symmetry of the container and is directed upwards, namely in the opposite direction to the gravity. Since the meniscus configuration has rotational symmetry, the further investigation is restricted to the semi-plane $\theta = 0$.

The static configuration of the meniscus is governed by the Young-Laplace equation,

$$\sigma\kappa = p_g - p_l \qquad \text{on } S_f, \tag{1}$$

where σ is the surface tension of the liquid, κ is the curvature of the meniscus, p is the hydrostatic pressure, and the subscripts $_g$ and $_l$ refer to the gas and the liquid phases respectively. The hydrostatic pressure distributions within the gas and the liquid are given by

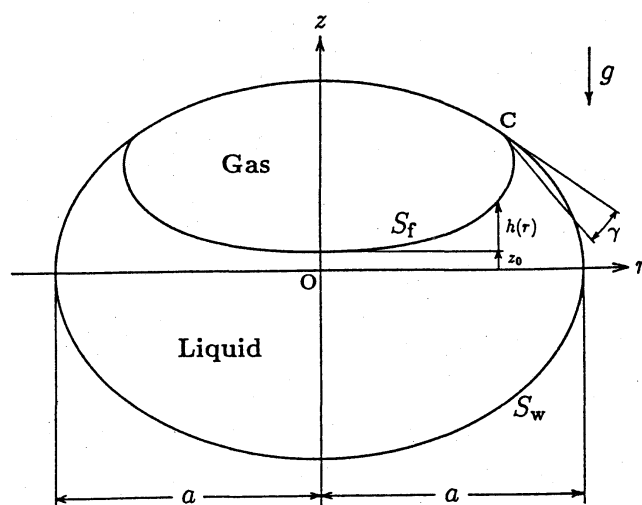$$p_g = p_g^0 - \rho_g g(z - z_0), \qquad p_l = p_l^0 - \rho_l g(z - z_0) \tag{2}$$

Fig. 1. A meniscus in a spheroidal container under low gravity

respectively. Here ρ is the density, g is the acceleration due to gravity, and p^0 is the pressure at a reference point of the height z_0 on S_f. In the present formulation, the reference point coincides with the intersection of the meniscus and the z-axis. Substituting the expression (2) into Eq. (1) yields

$$\sigma\kappa - \rho g h - \sigma\kappa_0 = 0, \tag{3}$$

with $\rho = \rho_l - \rho_g$ and $h = z - z_0$. Here $\kappa_0 = (p_g^0 - p_l^0)/\sigma$ denotes the curvature of the meniscus at the reference point.

It will be convenient to express all quantities in nondimensional form. Let the maximum semi-width of the container, a, be chosen as a representative length and set

$$R = \frac{r}{a}, \quad Z = \frac{z}{a}, \quad Z_0 = \frac{z_0}{a}, \quad H = \frac{h}{a}, \quad K = \kappa a, \quad K_0 = \kappa_0 a. \tag{4}$$

Then Eq. (3) becomes

$$K - Bo\,H - K_0 = 0, \tag{5}$$

where $Bo = \rho g a^2/\sigma$ is the Bond number which denotes the ratio of the gravitational force to the capilary force of the liquid. In the present formulation we employ the expression

$$K = R_s H_{ss} - H_s R_{ss} + \frac{H_s}{R}, \tag{6}$$

for the curvature K, where the parameter s is the nondimensional arc length measured along S_f from the reference point and the subscript s means the differentiation with respect to s. Then, $R(s)$ and $Z(s)$ ($= H(s) + Z_0$) give the nondimensional coordinates of points which form the meniscus S_f. Substituting the expression (6) into Eq. (5) yields

$$R_s H_{ss} - H_s R_{ss} + \frac{H_s}{R} - Bo\,H - K_0 = 0. \tag{7}$$

On the other hand, by differentiating the geometric relation

$$R_s^2 + H_s^2 = 1 \tag{8}$$

with respect to s, we obtain

$$R_s R_{ss} + H_s H_{ss} = 0. \tag{9}$$

From Eqs. (7) and(9), R_{ss} and H_{ss} are expressed as follows:

$$R_{ss} = -\lambda H_s, \quad H_{ss} = \lambda R_s, \tag{10}$$

where

$$\lambda = K_0 + Bo\,H - \frac{H_s}{R}. \tag{11}$$

As noticed by Concus et al.[2], a couple of differential equations (10) can be transformed into the following system of differential equations of the first order:

$$
\begin{aligned}
R_s &= U \\
H_s &= V \\
U_s &= -\lambda V \\
V_s &= \lambda U
\end{aligned}
\tag{12}
$$

It should be noticed here that the coefficient λ is a function of R, H and V as shown in Eq. (11).

The system of equations (12) is solved as an initial-value problem with the initial conditions

$$
R = H = V = 0, \quad U = 1 \quad \text{at } s = 0.
\tag{13}
$$

Moreover the problem is subjected to the subsidiary condition

$$
U^2 + V^2 = 1 \quad \text{for } s > 0
\tag{14}
$$

and the static contact-angle condition on the contact line C. The contact-angle condition is formulated as

$$
\theta_w - \theta_f = \gamma \quad \text{on C}
\tag{15}
$$

where θ_w is the angle between the radial direction and the tangent to the container wall, and θ_f is the angle between the radial direction and the tangent to the meniscus. Throughout the computaions in the present work, the contact angle is set as $\gamma = 5$ degrees.

3. Menisci in Spheroidal Containers

3.1. Computational strategy

The cross-section of a spheroidal container is expressed as

$$
R^2 + \frac{Z^2}{B^2} = 1
\tag{16}
$$

where B is the nondimensional length of the polar semi-axis of the container. It is noted here that the nondimensional length of the equatorial semi-axis is unity. The system of differential equations (12) is integrated numerically by the fourth-order Runge-Kutta method. For the practical use, the condition (15) is replaced with

$$
|\theta_f^n + \gamma - \theta_w^n| \le \varepsilon
\tag{17}
$$

by introducing a permissible small error limit ε. Throughout the present work, ε is taken to be 10^{-5}.

For fixed values of K_0 and Bo, the solution of Eq. (12) under the conditions (13), (14) and (17) proceeds in the following steps:

1. By assuming $Z_0 = 0$, the numerical integration of Eq. (12) is started from the origin O. The subsidiary condition (14) is satisfied by normalizing U and V as

$$U' = \frac{U}{\sqrt{U^2 + V^2}}, \qquad V' = \frac{V}{\sqrt{U^2 + V^2}} \tag{18}$$

and replacing U and V with U' and V' whenever U and V are evaluated during the integration.

2. Suppose that the numerical integration of Eq. (12) yields the radius R^n and the height Z^n of the point P^n at n-th step. Here the superscript n means that the quantities and the symbol refer to the position $s = n\,\Delta s$. Then, we calculate the angles θ_f^n and θ_w^n shown in Fig. 2 at the station $R = R^n$. If those angles satisfy the approximate contact-angle condition (17), all the points up to the point P^n are slided upwards or downwards along the Z-axis so that the point P^n comes to lie on the meridian of the container. If all the points are entirely within the domain surrounded by the ellipse expressed by Eq. (16), the curve formed by those points gives the meridian of a meniscus. It is obvious that the height Z_0 of the reference point is equal to the distance of movement of those points.
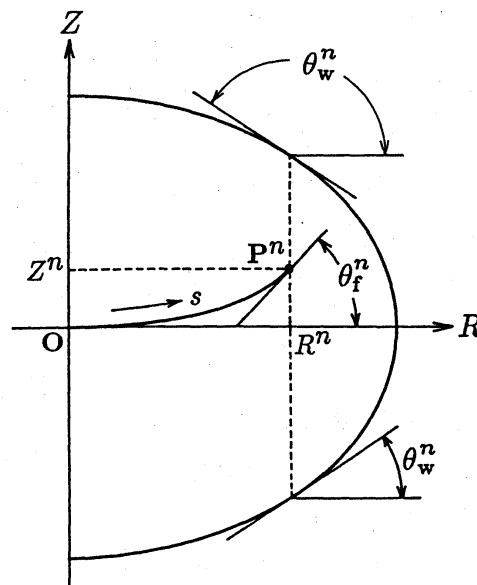

Fig. 2. Symbol definitions

3. If the condition (17) does not hold and the sign of $(\theta_f^n + \gamma - \theta_w^n)$ is different from that of $(\theta_f^{n-1} + \gamma - \theta_w^{n-1})$, this means that the contact point C exists between $R = R^{n-1}$ and $R = R^n$. Then the integration procedure is repeated in the interval of $R^{n-1} < R < R^n$ using a smaller increment than Δs. If the condition (17) does not hold and the sign of $(\theta_f^n + \gamma - \theta_w^n)$ is unchanged, the numerical integration progresses forward.

4. The volume Q of a liquid contained in the container is given as a resultant quantity. It is calculated by

$$Q = Q_1 + Q_2 \tag{19}$$

where Q_1 denotes the volume included between the meniscus and the horizontal plane $Z = Z_0$, and Q_2 denotes the volume between the container wall and the plane $Z = Z_0$. The volume Q_1 is expressed as

$$Q_1 = \int_{Z_0}^{Z_C} \pi(\hat{R}^2 - R^2)\, dZ \tag{20}$$

where Z_C is the height of the contact point C, and $\hat{R}$ and R are the radii of the container wall and the meniscus at height Z. The integration of Eq. (20) can be performed numerically. The volume Q_2 can be evaluated analytically using Eq. (16).

5. Repeat the steps 1-3 to obtain other possible profiles of menisci. The computation is continued until R exceeds unity or the angle θ_f exceeds π. As to be mentioned later, there are some cases in which three different menisci are computed for the fixed values of Bo and K_0.

To start the computation we must evaluate λ at $s = 0$. In three-dimensional cases, however, it is difficult to calculate straightforwardly the initial value of λ, since the expression of λ includes the term H_s/R and R vanishes at $s = 0$. Then analytical considerations are required. By using L'Hospital's Rule, the term H_s/R can be evaluated at $s = 0$ as follows:

$$\left(\frac{H_s}{R}\right)_{s=0} = \lim_{s \to 0} \frac{H_s}{R} = \lim_{s \to 0} \frac{H_{ss}}{R_s} = (H_{ss})_{s=0}. \tag{21}$$

Applying Eq. (7) to the point $s = 0$ together with the initial condition (13) and the relation (21), we obtain

$$\left(\frac{H_s}{R}\right)_{s=0} = \frac{K_0}{2}. \tag{22}$$

Then λ is evaluated at $s = 0$ as

$$(\lambda)_{s=0} = K_0 - \frac{K_0}{2} = \frac{K_0}{2}. \tag{23}$$

To verify the computational accuracy, we have first calculated meniscus profiles in three-dimensional circular cylindrical and two-dimensional rectangular containers for which analytical exact solutions are available[6]. Good agreement has been obtained between numerical and analytical solutions. The details can be found in Ref. 7.

3.2. Meniscus profiles for given values of K_0

For given values of Bo and K_0, the problem has not necessarily a unique solution. When $Bo = 50$ and $K_0 = 0.0631$, for example, three different profiles of menisci are obtained in a spherical container as shown in Fig. 3. The corresponding volume fractions of the liquid relative to the container volume are 1.2008×10^{-5}, 0.135 and 0.647.

Here we refer to the least volume, 1.2008×10^{-5}. The above results correspond to $\Delta s = 0.01$, where Δs is the step size of the numerical integration and denotes the segment length of the meridian of the meniscus. The calculation of the liquid volume uses the same segment division as in the numerical integration. In the above computation, the meridian of the meniscus corresponding to the least volume has been divided into 12 segments. A finer division of 902 segments with $\Delta s = 10^{-4}$ has yielded the least volume of 1.2002×10^{-5}. From these results, we come to the conclusion that the value of 1.2008×10^{-5} has never been yielded by numerical errors and it gives the amount of liquid volume. Although the solution corresponding to the least liquid volume is meaningful mathematically, it is not so significant for practical purposes.
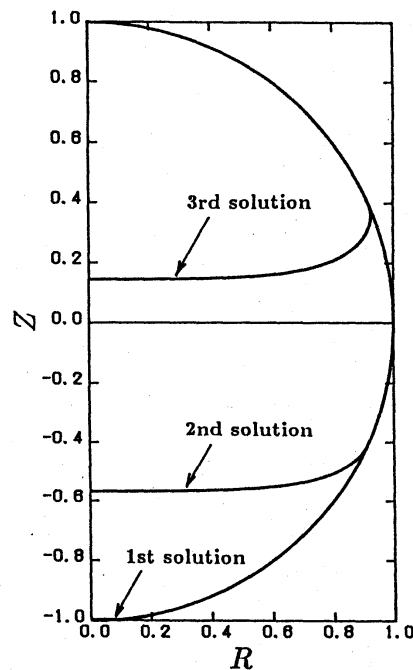

Fig. 3. Three solutions of meniscus profiles in a spherical container ($Bo = 50$, $K_0 = 0.0631$)
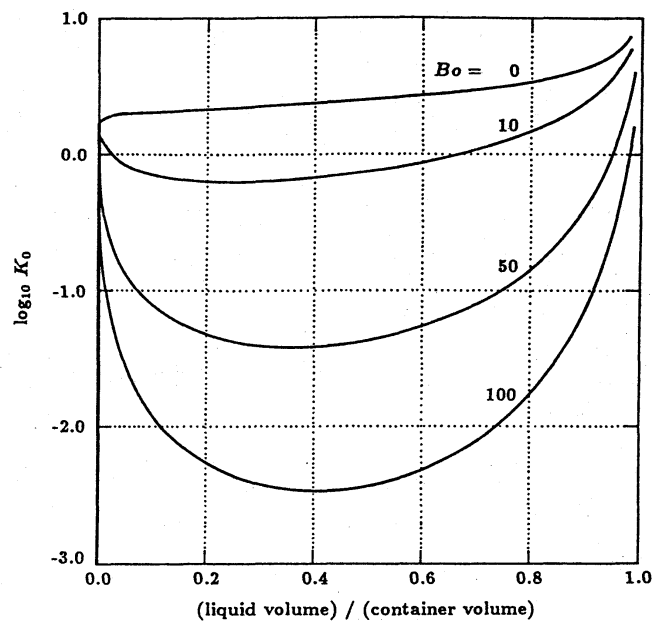
Fig. 4. Relations between liquid-volume fraction and $\log_{10} K_0$ for different Bond numbers

The systematic calculation of liquid volume for different values of K_0 gives the relation between K_0 and liquid volume for the given shape of a container and a given Bond number. Figure 4 shows the relations obtained in a spherical container for $Bo = 0, 10, 50, 100$. The abscissa denotes the liquid-volume fraction which is defined as liquid volume devided by container volume, and the ordinate denotes the logarithmic value of K_0. It is found that for each Bond number except $Bo = 0$, there is a range of K_0 in which three different amounts of volume are possible for a fixed value of K_0 and the range shortens as the Bond number decreases. In the case of $Bo = 0$, the liquid volume is a single-valued function of K_0.

3.3. Meniscus profiles for given liquid volume

In most practical cases in engineering field, meniscus profiles will be required for pre-scribed amounts of liquid volume contained in a vessel, not for given values of K_0. Rough computations may be made by estimating values of K_0 corresponding to given liquid volume on a chart as Fig. 4. For detailed calculations, iterative solution algorithms should be prepared.

In the present work, a Newton-like iterative method is used. The process proceeds as follows:

1. Suppose that two different amounts of liquid volume, Q_i and Q_{i+1}, are calculated for the values K_0^i and K_0^{i+1} of K_0, respectively. Here sub- and superscript i and $i + 1$ denote the step number in iterations. Since three different amounts of liquid volume are generally obtained against a fixed value of K_0, the closest amount of volume to the prescribed volume Q^* should be chosen among the three.

2. Estimate the $(i+2)$-th approximation of K_0 by

$$K_0^{i+2} = \frac{K_0^{i+1} - K_0^i}{Q_{i+1} - Q_i}(Q^* - Q_{i+1}) + K_0^{i+1} . \tag{24}$$

Then compute liquid volume Q_{i+2}. If $|Q^* - Q_{i+2}|$ is less than or equal to a given permissible error, the corresponding profile of meniscus is the desired one. If not, try again the steps 1 and 2 using K_0^{i+1} and K_0^{i+2}.

The initial guess for K_0 can be obtained using a chart of liquid volume versus K_0 similar to Fig. 4.

Figures 5 and 6 show meniscus profiles of liquid with different volume fractions in a spherical container, and Figures 7 and 8 show those in the spheroidal container of $B = 0.6$. In each figure, prescribed and computed liquid-volume fractions and values of K_0 corresponding to computed profiles of menisci are tabulated. In Fig. 7, the menisci corresponding to the liquid-volume fractions of 0.50, 0.25 and 0.10 have not been obtained, since the meridian of the meniscus does not wholly lie within the container. This may mean that the liquid cannot exist in a simply connected domain as shown in Fig. 1 and separates into two crescent-shaped regions.

Meniscus	Prescribed volume fraction	Computed volume fraction	Corresponding value of K_0
A	0.950	0.949944	5.4268
B	0.750	0.750000	3.1746
C	0.500	0.500037	2.5189
D	0.250	0.250007	2.1954
E	0.100	0.100004	2.0433

Meniscus	Prescribed volume fraction	Computed volume fraction	Corresponding value of K_0
A	0.950	0.949994	0.2683
B	0.750	0.749942	0.0110
C	0.500	0.500003	0.0037
D	0.250	0.250000	0.0044
E	0.100	0.100000	0.0119

Fig. 5. Meniscus profiles corresponding to different liquid-volume fractions in a spherical container ($Bo = 0$)
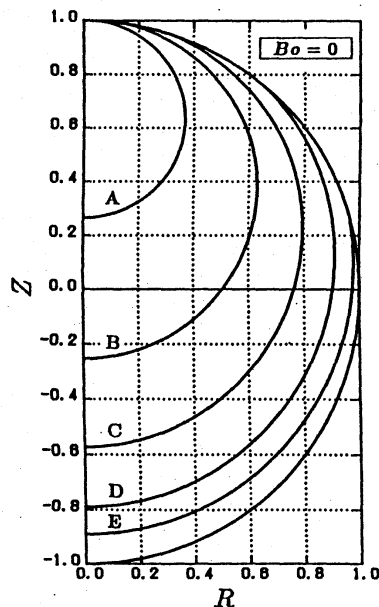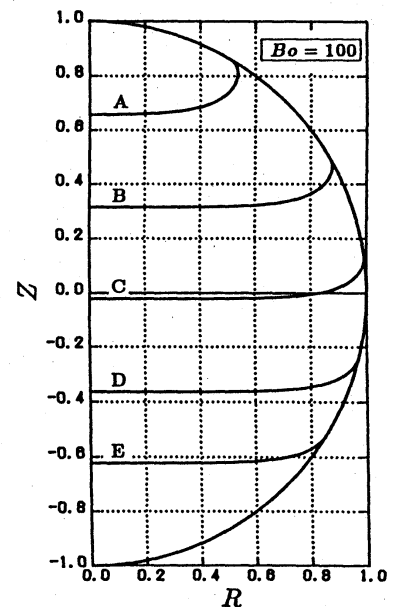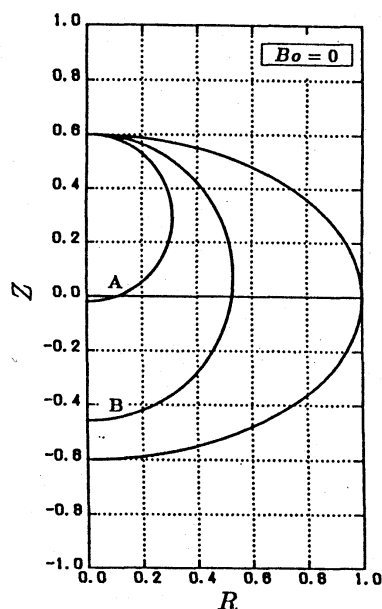
Fig. 6. Meniscus profiles corresponding to different liquid-volume fractions in a spherical container ($Bo = 100$)

Meniscus	Prescribed volume fraction	Computed volume fraction	Corresponding value of K_0
A	0.950	0.949997	6.4364
B	0.750	0.749984	3.7640
C	0.500	(not obtained)	
D	0.250	(not obtained)	
E	0.100	(not obtained)	

Meniscus	Prescribed volume fraction	Computed volume fraction	Corresponding value of K_0
A	0.950	0.949952	0.5536
B	0.750	0.749980	0.0185
C	0.500	0.499991	0.0044
D	0.250	0.249994	0.0038
E	0.100	0.099998	0.0086

Fig. 7. Meniscus profiles corresponding to different liquid-volume fractions in a spheroidal container ($Bo = 0$)
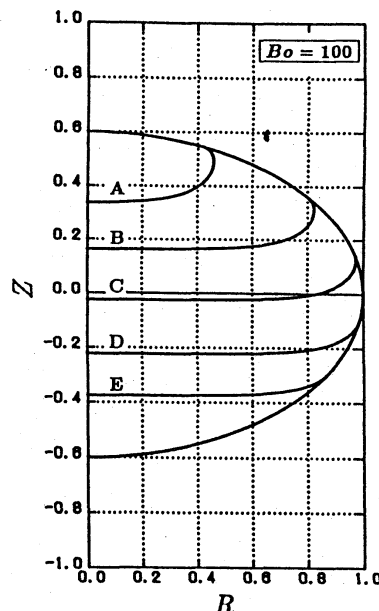

Fig. 8. Meniscus profiles corresponding to different liquid-volume fractions in a spheroidal container ($Bo = 100$)

4. Application to the Calculation of Droplet Configurations

The present method is applied to the calculation of configurations of droplets on a horizontal flat plate. The droplet configuration is assumed to have rotational symmetry around a vertical axis. The computed profiles of meridians of free surfaces are shown in Fig. 9. In these calculations, the radius of a contact line on the plate is chosen as a representative length used in the nondimensionalization of quantities. The calculation prcedure goes as follows:

1. Specify the Bond number and assume the value of K_0. In the present problem, K_0 should have a negative value. Then, start the numerical integration from the origin O and continue it until the contact-angle condition is satisfied.

2. Examine whether the calculated radius of a contact line is unity or not. if it is equal to unity within a prescribed permissible error, the calculation is stopped. Otherwise, the steps 1 and 2 are repeated with other value of K_0.
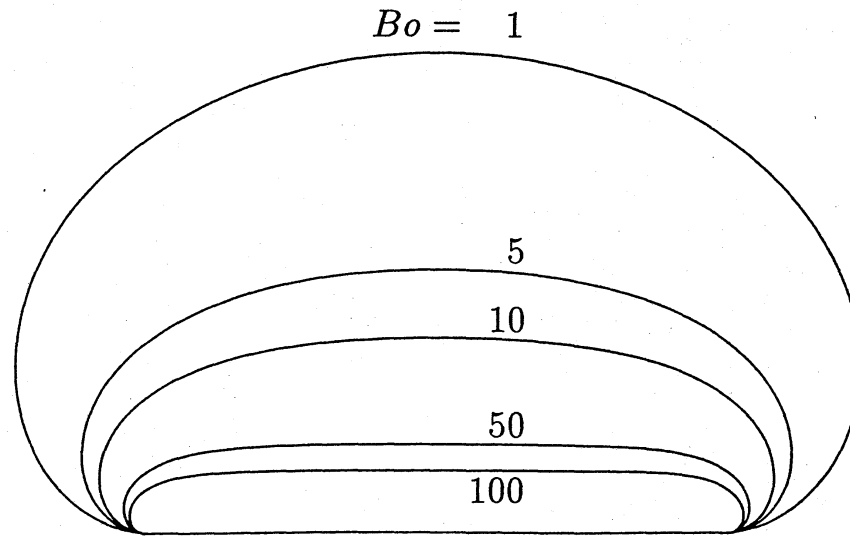
Fig. 9. Droplet profiles for different Bond numbers

The computed results in Fig. 9 correspond to $\gamma = 175$ degrees.

In the case of inclined flat plates, the problem will become more difficult. It will be a challenging subject for us in the future.

5. Concluding Remarks

Numerical studies concerning axisymmetric configurations of free liquid surfaces in low-gravity environment have been carried out. As an illustrative example, meniscus configurations in spheroidal containers have been used to describe the methodology. The meridian profiles of menisci have been obtained as solutions of the Young-Laplace equation, which has been transformed into a system of four ordinary differential equations and integrated numerically by the Runge-Kutta method. The system of equations includes an arbitrary constant K_0, and liquid volume contained within a vessel is determined as a resultant quantity for a prescribed value of K_0. When liquid volume is given on the contrary, difficulties occur with respect to the determination of K_0. Then, we have made clear graphically the relations between liquid volume and K_0 by the implementation of the systematic calculations of liquid volume against K_0. Furthermore, based on those relations, an iterative numerical scheme is developed for determining a meniscus profile with prescribed liquid volume.

References

1) Neu, J. T. and Good, R. J.: Equilibrium Behavior of Fluids in Containers at Zero Gravity, AIAA Journal, 1(1963), pp. 814-819.

2) Concus, P., Crane, G. E. and Satterlee, H. M.: Small Amplitude Lateral Sloshing in Spheroidal Containers under Low Gravitational Conditions, NASA CR-72500, 1969.

3) Komatsu, K.: Liquid Sloshing in Spacecraft (in Japanese), Journal of the Japan Society for Aeronautical and Space Sciences, 34(1986), pp. 461-469.

4) Utsumi, M. and Kondo, H.: Liquid Sloshing in a Spherical Container at Low-Gravity Environments (1st report, Static Configuration of Liquid Surface)(in Japanese), Transactions of the Japanese Society of Mechanical Engineers, 53(1987), 1683-1689.

5) Schilling, U. and Siekmann, J.: Numerical Study of Equilibrium Capillary Surfaces under Low Gravitational Conditions, Ingenieur-Archiv, 60(1990), pp. 176-182.

6) Ono, A.: Surface Tension (in Japanese), Kyoritsu Shuppan, Tokyo, 1980.

7) Nakayama, T.: Static Meniscus Configurations in Axisymmetric Containers under Low-gravity Conditions, to appear in Transactions of the Japan Society for Aeronautical and Space Sciences (1992).